

Mesoscopic two-mode entangled and steerable states of 40,000 atoms in a Bose-Einstein condensate interferometer

B. Opanchuk¹, L. Rosales-Zárate², R. Y. Teh¹, B. J. Dalton^{1,3}, A. Sidorov¹, P. D. Drummond^{1,4} and M. D. Reid^{1,4}

¹*Centre for Quantum and Optical Science Swinburne University of Technology, Melbourne, Australia*

²*Centro de Investigaciones en Óptica A.C., León, Guanajuato 37150, México*

³*Centre for Cold Matter, Blackett Laboratory, Imperial College of Science, Technology and Medicine, London SW7 2BZ, United Kingdom and*

⁴*Institute of Theoretical Atomic, Molecular and Optical Physics (ITAMP), Harvard University, Cambridge, Massachusetts, USA*

Using criteria based on superselection rules, we analyze the quantum correlations between the two condensate modes of the Bose-Einstein condensate interferometer of Egorov et al. [Phys. Rev. A **84**, 021605 (2011)]. In order to determine the two-mode correlations, we develop a multi-mode theory that describes the dynamics of the condensate atoms and the thermal fraction through the interferometer sequence, in agreement with the experimentally measured fringe visibility. We thus present experimental evidence for two-mode entangled states genuinely involving 40,000 ⁸⁷Rb atoms, and for two-way steerability between two groups of 20,000 indistinguishable atoms.

In the Einstein, Podolsky and Rosen (EPR) paradox, a measurement made by an observer at one location can apparently instantaneously affect the quantum state at another [1]. This effect was called “steering” by Schrodinger [2, 3]. States that give the correlations of an EPR paradox are called steerable, or EPR steerable if the two locations are spatially separated [3–6]. Although well verified for optical systems [7, 8], it is a challenge to demonstrate EPR steering correlations between large massive systems. To resolve paradoxes associated with macroscopic quantum objects, decoherence theories propose to modify quantum mechanics by including gravitational effects [9, 10], thus distinguishing between massive and massless systems. For these reasons, the detection of EPR steering correlations between mesoscopic groups of atoms is an important milestone.

There has been success in entangling massive systems [11–19]. Yet entanglement does not imply steering, which is a stronger form of quantum correlation. Steering is a necessary (though not sufficient) requirement for all systems that show Bell-nonlocality [20], and is useful for certain quantum information tasks [21]. Several experimental groups have inferred Bell or steering correlations between atoms within an atomic ensemble [11–13], and there has been demonstration of Bell correlations involving optomechanical oscillators [22]. In a further step, EPR steering has been observed between spatially separated clouds of several hundreds of atoms formed from a Bose-Einstein condensate (BEC) [14, 15, 19].

However, there is a difference between states with many mutually entangled atoms, and states built of multiple smaller entangled units, such as independent pairs of entangled atoms. This distinction has motivated experiments that rigorously quantify the number of atoms genuinely involved in the entangled unit (called the “depth of entanglement” [23, 24]), leading to evidence of states

with a few hundred atoms mutually entangled in a BEC [25, 26], a few thousand in a thermal atomic ensemble [27], and up to a few million in a crystal lattice [28]. However, entanglement does not imply steering, and so far atomic experiments have not addressed the size of steerable units. Moreover, most experiments have considered entanglement shared between distinguishable particles. This contrasts with a BEC, where atoms are indistinguishable particles occupying distinct modes. Since modes can be separated, demonstrating mode entanglement for highly occupied modes is promising for obtaining nonlocality between spatially separated mesoscopic groups of atoms. While mode entanglement has recently been observed [14, 15, 19], the maximum number of atoms involved has been limited to several hundred.

In this paper, we present experimental evidence for atomic two-mode steerable entangled states genuinely involving 40,000 atoms, with 20,000 atoms localised in each condensate mode. The states are created in a multi-mode ⁸⁷Rb BEC Ramsey interferometer of $\sim 55,000$ atoms at a temperature of $\sim 37nK$ and prepared on an atom chip in a magnetic trap [29, 30]. Steering is a directional form of entanglement, because one can consider a nonlocal effect one way, on one system due to measurements on the other, and vice versa. Two-way steering is required for Bell nonlocality [3, 5]. Here, we demonstrate that the correlations between two atomic condensate modes are two-way steerable, thereby inferring the steerability of 20,000 indistinguishable atoms.

It is important to clarify the meaning of “entangled states genuinely involving N atoms”, in the context of mode entanglement. The entanglement depth is not simply the number of atoms in the experiment, nor the number of atoms in the two condensate modes. This is because the system may be in a mixed state where large numbers of atoms are in separable (non-entangled) two-

mode states. Furthermore, at finite temperature, a significant number of atoms are lost into thermal modes. We define the “mode-entanglement (steering) depth” as the number of atoms N in the part of the density operator associated with two-mode entanglement (steering). Specifically, we will confirm that the entanglement cannot be explained, if we allow that the number N is reduced. In this paper, we measure a mode-entanglement and mode-steering depth of 40,000 atoms.

Mode versus particle entanglement: We may ask how to compare the mode-entanglement depth with the particle-entanglement depth investigated in previous experiments. Indeed, there has been controversy about the meaning of particle entanglement when particles are indistinguishable, and hence not individually localisable, as in a BEC [31–33].

To illustrate, consider bosons incident on a Ramsey BEC interferometer. For two atomic bosonic modes, superselection rules apply that fix the total particle number N for a pure state [31, 34–37]. The most general pure two-mode state is then of the form (\mathcal{N} is a constant)

$$|\psi_N\rangle = \mathcal{N} \sum_{n=0,1,\dots}^N d_n \sqrt{\binom{N}{n}} |n\rangle_a |N-n\rangle_b \quad (1)$$

where d_n are complex amplitudes. Here $|n\rangle_a |N-n\rangle_b$ denotes n particles in mode a with spin 0, and $N-n$ particles in mode b with spin 1. The state is mode-entangled for any d_n , provided $d_n \neq 0$ for at least two values of n . Following [32], we write $|n\rangle |N-n\rangle = \frac{1}{\sqrt{\binom{N}{n}}} S |0\rangle_1 \dots |0\rangle_n |1\rangle_{n+1} \dots |1\rangle_N$ where S denotes symmetrisation of the particle state in first quantisation [32]. If we view the pseudo-labels $1, \dots, N$ of the symmetrised wave function as corresponding to N distinguishable particles, then it is straightforward to show that the mode-separable state $|n\rangle_a |N-n\rangle_b$ for $n = 1, \dots, N-1$ is both N -particle entangled and N -particle steerable [38–40]. This is also true in general for the mode-entangled state $|\psi_N\rangle$, except for some singular choices such as $d_n = 1$. Details are given in the Supplemental Materials [40, 41].

This provides a link between the mode-entanglement depth, and the pseudo-label particle-entanglement depth inferred in earlier experiments [25, 26]: A two-mode entangled state with a mode-entanglement (steering) depth of N is also pseudo-label particle-entangled (steerable) with depth N , except in the singular cases. In those cases, once we determine the value N of the mode-entanglement (steering) depth, a state with pseudo-label N -particle entanglement (steering) can be prepared by a local operation that projects onto a definite local mode number n [31]. Although this N -particle entanglement is without operational meaning (since pseudo-labelled systems are not independently measurable [31–33, 42]), such particle entanglement can be transformed into multipartite mode entanglement by expanding and splitting

the BEC [14, 15, 32]. An N -partite entanglement can only be realised however, once each atom is localisable.

The observation of any degree of spin squeezing is sufficient to imply a (pseudo-label) N -particle entanglement, once the mode-entanglement depth N has been determined. This follows because the particles are indistinguishable [40]. In our experiment, a spin squeezed state $|\psi_N\rangle$ is predicted as the atoms evolve [40], but we do not measure this effect. In fact, $|\psi_N\rangle$ with $d_n = 1$ is an approximate model for the state generated. While such a state is separable with respect to the pseudo-labels, this has limited meaning because the subsystems are not distinguishable. In particular, if we envisage preparing each atom independently in its own mode to ensure localisation (with each split equally between a and b), then, because the atoms are indistinguishable, the resulting symmetrised wave function in the coordinate representation is not factorisable with respect to the N modes [31]. Most relevant is that the operational entanglement between a and b as measured by the entropy of entanglement is of order N (or $\frac{1}{2} \log N$ for $|\psi_N\rangle$ with $d_n = 1$), illustrating a cooperative effect due to all N bosons (refer to the Supplemental Materials for details of the proofs) [31, 40].

Steering: We begin by defining the concept of steering for two systems a and b [3]. Where each system is a single mode, we introduce boson creation and destruction operators \hat{a}^\dagger , \hat{a} , \hat{b}^\dagger , \hat{b} for a and b respectively. The two systems are entangled if the quantum density operator ρ of the composite system cannot be described according to a separable model $\rho = \sum_R P_R \rho_a^R \rho_b^R$. Here, ρ_a^R and ρ_b^R are density operators for a and b , and P_R are probabilities satisfying $\sum_R P_R = 1$ and $P_R > 0$. If the modes are at different locations, EPR steering of b by a is demonstrated if there is a failure of all local hidden state models, where the averages for locally measured observables X_a and X_b are given as [3, 4]

$$\langle X_b X_a \rangle = \int_\lambda P(\lambda) d\lambda \langle X_b \rangle_{\rho, \lambda} \langle X_a \rangle_\lambda \quad (2)$$

The states symbolized by λ are the hidden variable states introduced in Bell’s local hidden variable models, with probability density $P(\lambda)$ satisfying $\int_\lambda P(\lambda) d\lambda = 1$. $\langle X_a \rangle_\lambda$ is the average outcome of X_a given the system is in the state λ . The ρ subscript denotes that the average $\langle X_b \rangle_{\rho, \lambda}$ is generated from a local quantum state with quantum density matrix ρ_b^λ .

Entangled modes of an interferometer: The entangled states reported in this paper can be understood using a simple model of a Mach-Zehnder interferometer (Figure 1). Consider two field modes impinging on a 50/50 beam splitter $BS1$. The input state for mode a is a Fock number state $|N\rangle_a$ describing N bosons. The input to b is the vacuum state $|0\rangle_b$. The output of the beam splitter is the two-mode entangled state $|\psi_N\rangle$ (1) where $d_n = 1$, $\mathcal{N} = 1/\sqrt{2^N}$ [43]. Equivalent predictions are given for a BEC atom Ramsey interferometer.

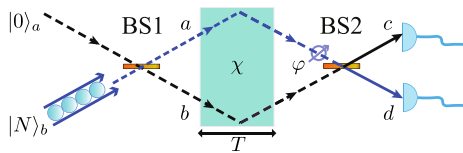


Figure 1. Schematic of a two-mode Mach-Zehnder interferometer. Entangled modes a and b are prepared by means of a number state $|N\rangle_a$ incident on the first beam splitter BS1. The entanglement may be enhanced by a nonlinear interaction χ acting for a time T .

The incident mode $|N\rangle$ represents N atoms of a single-component BEC prepared in an atomic hyperfine level $|1\rangle = |F=1, m_F=-1\rangle$ (spin 0). A $\pi/2$ microwave pulse creates a two-component BEC associated with two hyperfine levels $|1\rangle$ and $|2\rangle = |F=1, m_F=1\rangle$ (spin 1). This produces the action of the beam splitter BS1, creating the mode-entangled state $|\psi_N\rangle$. The components $|1\rangle$ and $|2\rangle$ correspond to well-defined spatial condensate modes a and b . The nonlinearity χ of the BEC gives rise to enhanced entanglement, and an N -particle entanglement with respect to particle pseudo-labels [23–26, 44–48]. After an evolution time T , a second interrogating microwave pulse is applied with a phase lag φ , producing the action of a second beam splitter. Immediately after, the atoms are released and the two-component population difference $\langle \hat{N}_- \rangle$ measured by atom imaging. The size of the moment $\langle \hat{a}^\dagger \hat{b} \rangle$ can be used to detect the entanglement between the modes [47, 49, 50]. It is difficult however to use existing criteria [24, 47, 49, 50], due to the difficulty of preparing a state with an exact atom number N .

Super-selection rules and criteria for steering: Two-mode entanglement and steering can regardless be inferred if the bosons are *atoms*, using an alternative two-mode criterion

$$\langle \hat{a}^\dagger \hat{b} \rangle \neq 0 \quad (3)$$

sufficient to confirm both entanglement and a two-way steering between modes a and b . The criterion is based on superselection rules that forbid superpositions of eigenstates of different single-mode atom number [31, 33–37, 51]. Following Refs. [34, 51], we give proof of the condition (3). The density operator for any separable state can be written $\rho = \sum_R P_R \rho_a^R \rho_b^R$. According to the superselection rule, the single-mode atom coherences $\langle \hat{a} \rangle_R$ and $\langle \hat{b} \rangle_R$ vanish, for any local single mode quantum states ρ_a^R and ρ_b^R . Thus, the separable model implies $\langle \hat{a}^\dagger \hat{b} \rangle = \sum_R P_R (\langle \hat{a} \rangle_R \langle \hat{b} \rangle_R) = 0$, as does the local hidden state model (2). Unless we allow that the individual modes violate the superselection rule, the observation of $\langle \hat{a}^\dagger \hat{b} \rangle \neq 0$ is sufficient to confirm entanglement, and a “two-way” steering (b by a , and a by b) between the modes.

Ultimately, we envisage detecting $\langle \hat{a}^\dagger \hat{b} \rangle \neq 0$ using localized measurements on each of the modes, in the spirit of the Einstein-Podolsky-Rosen argument [1]. This is possible using quadrature phase amplitudes $\hat{X}_a = \hat{a} + \hat{a}^\dagger$, $\hat{P}_a = (\hat{a} - \hat{a}^\dagger)/i$ and $\hat{X}_b = \hat{b} + \hat{b}^\dagger$, $\hat{P}_b = (\hat{b} - \hat{b}^\dagger)/i$, since one can expand $\langle \hat{a}^\dagger \hat{b} \rangle = (\langle \hat{X}_a \hat{X}_b \rangle + \langle \hat{P}_a \hat{P}_b \rangle - i \langle \hat{P}_a \hat{X}_b \rangle + i \langle \hat{X}_a \hat{P}_b \rangle)/4$ [11, 14, 18]. As a preliminary step to such an observation, we show that $\langle \hat{a}^\dagger \hat{b} \rangle \neq 0$ can be inferred, based on interferometry. Introducing a phase shift φ , the two-mode outputs of the interferometer are described by operators $\hat{c} = (\hat{a} - \hat{b} \exp^{i\varphi})/\sqrt{2}$, $\hat{d} = (\hat{a} + \hat{b} \exp^{i\varphi})/\sqrt{2}$. Defining $\hat{N}_\pm = \hat{d}^\dagger \hat{d} \pm \hat{c}^\dagger \hat{c}$ and assuming N_+ to be fixed, the normalized average population difference $P_z = N_-/N_+$ at the output is $P_z = 2(\text{Re}\langle \hat{a}^\dagger \hat{b} \rangle \cos \varphi - \text{Im}\langle \hat{a}^\dagger \hat{b} \rangle \sin \varphi)/N_+$ (N_\pm are the outcomes of \hat{N}_\pm). By adjusting φ , $|\langle \hat{a}^\dagger \hat{b} \rangle|$ can be inferred from the interference fringe amplitude ν , ($\nu = 2|\langle \hat{a}^\dagger \hat{b} \rangle|$) [29, 30, 40]. The observed fringe pattern for the BEC interferometer is given in Figure 2. While T and φ can be controlled experimentally, there are run-to-run fluctuations in the total atom number N_+ . The criterion $\langle \hat{a}^\dagger \hat{b} \rangle \neq 0$ is however valid for all mixed two-mode states and hence applies to fluctuating number inputs.

Depth of steering: We next address how to determine the number of atoms in the steerable unit – the “mode-steering depth n_{st} ” [24]. This is not given by the mean number $\langle N \rangle$ of particles because the system is generally a mixture of pure states $|\psi_R\rangle$, according to a density operator $\rho = \sum_R P_R |\psi_R\rangle \langle \psi_R|$ ($\sum_R P_R = 1, P_R > 0$). While laboratory preparations of a BEC are near-pure states, a mixed state analysis is required because of finite temperatures and fluctuations in the atom number. Each pure state $|\psi_R\rangle$ has a fixed number of atoms (according to superselection rules) that we denote by $n_R = \langle \psi_R | N | \psi_R \rangle$. However, not all the $|\psi_R\rangle$ need be steerable. Defining n_{st} to be the maximum value of n_R

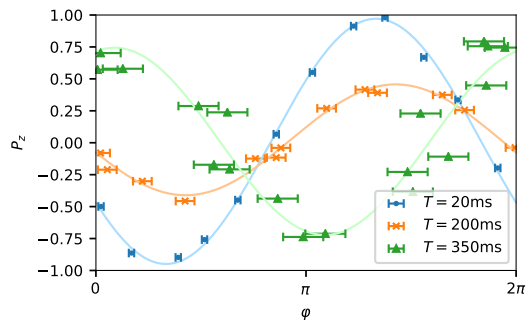


Figure 2. The plot shows the experimentally observed interference at $T = 20\text{ms}$, $T = 200\text{ms}$, $T = 350\text{ms}$. The $P_z = N_-/N_+$ is the normalized population difference after a correction $\phi(N_+, T)$ is added as explained in Refs. [29] to account for the effect of fluctuating population number N_+ . Here $N_+ \sim 10^4$ atoms. The solid line is the best fit to the data. The observed fringe amplitude is larger than predicted by a two-mode model, due to the presence of thermal atoms.

taken over all the $|\psi_R\rangle$ that are steerable, we prove in the Supplementary Materials that [40]

$$n_{st} \geq 2|\langle \hat{a}^\dagger \hat{b} \rangle| \quad (4)$$

We might apply the criterion to known experimental systems e.g. the creation of two steerable modes is possible for a BEC in a double-well potential [46, 47]. In order to properly quantify the two-mode correlation $\langle \hat{a}^\dagger \hat{b} \rangle$ for larger BECs, however, a full multi-mode model is necessary. This is particularly true for higher temperatures, and is necessary because the extra modes involving thermal atoms contribute to the measured fringe contrast. Some atom interferometers have large fringe visibilities and yet comprise multiple thermally-excited modes, with a small occupation of each mode (see Refs. [13, 52, 53]).

Multi-mode BEC interferometer: To infer a steerable state of thousands of atoms, we calculate the condensate fractions in the BEC interferometer using the Onsager-Penrose criterion [54]. The quantum dynamics are evaluated using a multi-mode field-theoretic phase-space method based on the Wigner function [29, 55]. The effective Hamiltonian for the two-mode condensate system is [44, 45, 55–57]:

$$\hat{H} = \int d^3\mathbf{x} \sum_{k,j=1}^2 \left\{ \hat{\Psi}_i^\dagger K_{ij} \hat{\Psi}_j + \frac{g_{ij}}{2} \hat{\Psi}_i^\dagger \hat{\Psi}_j^\dagger \hat{\Psi}_i \hat{\Psi}_j \right\}, \quad (5)$$

where $\hat{\Psi}_j$ describes a bosonic quantum field operator with internal spin orientation labelled $j = 1, 2$ for the two levels $|1\rangle, |2\rangle$ (corresponding to spin states $|0\rangle$ and $|1\rangle$). Here $g_{jk} = 4\pi\hbar^2 a_{jk}/m$ gives the S-wave scattering interaction strength, and the single-particle Hamiltonian operator is $K_{ij} = (-\hbar^2\nabla^2/2m + V(\mathbf{x}))\delta_{ij} + \hbar\Omega_{ij}(t)$. The important terms are the atomic mass m , a trap potential $V(\mathbf{x}) = m\sum_j \omega_j^2 x_j^2/2$ and an inter-level Rabi cycling matrix Ω_{ij} . Previous work calculating a static condensate fraction used both the semiclassical Hartree-Fock (SHF) approximations and Monte-Carlo methods [58], showing excellent agreement of these methods in thermal equilibrium, far from the critical point. This has also been accurately verified experimentally [59].

To obtain the initial density matrix $\rho_{initial}$ we use the SHF method. This describes the initial finite temperature ensemble of a three-dimensional, trapped BEC as a coherent condensate $\phi_j(\mathbf{x})$ surrounded by a thermal cloud with occupation $n_j^{(T)}(\mathbf{x})$ (Fig. 3). The thermal fraction density $n^{(T)}$ and the condensate fraction density $n^{(c)} \equiv |\phi|^2$ for the first component are found self-consistently.

Since the state is no longer in thermal equilibrium after the action of the first beam splitter, the condensate evolves dynamically until rotated back to finish the experiment. To solve the evolution, it is necessary to

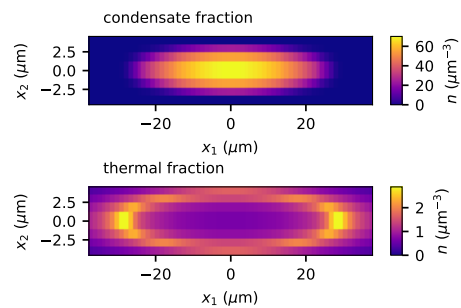


Figure 3. The three-dimensional model gives details of the initial condensate fraction along the axial coordinates of the interferometer. The slices shown are taken along the long axis of the trap, and give the densities of the initial condensate (lower) and thermal (top) fractions. The total atom population (thermal and BEC fractions) is 55000. The initial total condensate population is $N = 48325$.

go beyond Hartree-Fock approximations. Due to thermal atoms which form a halo around the central condensate at finite temperature (Fig. 3), there are large numbers of field modes participating both in the initial quantum ensemble and its evolution, as well as atomic losses. To model these effects, the quantum field dynamics is mapped into a phase-space using a master equation and truncated Wigner approximation valid at large atom number N [60–62]. Each quantum field $\hat{\Psi}_j$ is transformed into an equivalent ensemble of complex stochastic fields ψ_j , that obey a stochastic partial differential equation which is numerically solved.

The initial condition is assumed to be a grand canonical ensemble in one of the two components, with an approximately Poissonian number distribution. For com-

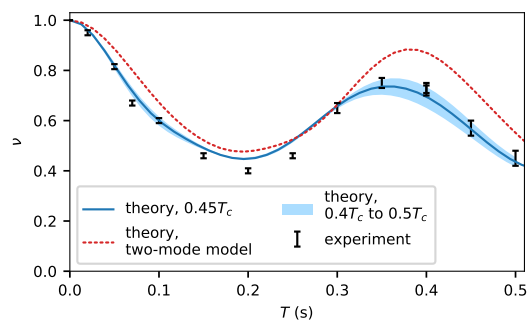


Figure 4. The black points give the experimentally observed fringe contrast ν versus the evolution time T . The blue curve is the fringe visibility predicted by the multimode theoretical model. The initial temperature is $T_{BEC} = 0.45T_c$ where T_c is the critical temperature at which the atoms form a condensate. The red line shows visibilities obtained with the assumption of a zero-temperature two-mode model. The thickness of the blue curve corresponds to the range produced from the values $T = 0.4T_c$ and $T = 0.5T_c$ to demonstrate the error due to the initial temperature estimate.

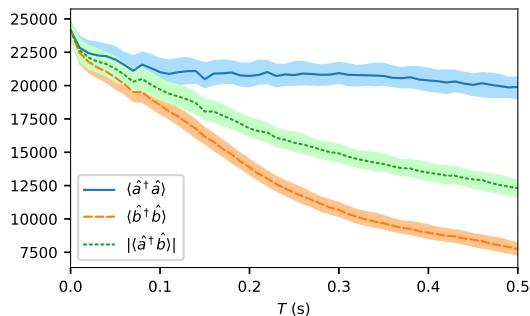


Figure 5. The curves show the number of atoms $\langle \hat{a}^\dagger \hat{a} \rangle$ and $\langle \hat{b}^\dagger \hat{b} \rangle$ in the condensate modes a and b of each atomic component, and the two-mode moment $\langle \hat{a}^\dagger \hat{b} \rangle$, inferred from the model. The curves in each pair correspond to the values $T = 0.4T_c$ and $T = 0.5T_c$ to demonstrate the error due to the initial temperature estimate.

parison purposes, we consider two initial states. In one of the plotted lines of Figure 4, we use a coherent state with average density equal to the solution of the mean-field Gross-Pitaevskii equation.

The absolute temperature is obtained by fitting to the observed fringe visibility (Fig. 3). This yields an upper bound to the temperature, expressed as a fraction of the ideal gas critical temperature T_c at the same atom number, since there are other technical noise effects that may slightly degrade the visibility as well. We find $T_{BEC} = (0.45 \pm 0.05)T_c \approx 37nK$, where $T_c = (\hbar\bar{\omega}/k_B) (N/\zeta(3))^{1/3} \approx 83nK$ is the nominal critical temperature below which the BEC starts to form for a noninteracting gas with mean trap frequency $\bar{\omega} = (\omega_1\omega_2\omega_3)^{1/3}$.

Our model includes the spatial evolution of the wave functions, and thus accounts for the experimentally observed oscillation of the fringe visibility as a function of T (Fig. 4). One mode decays more quickly due to inelastic scattering (Fig. 5). Interatomic repulsion is larger for different states, leading to the fringe visibility oscillation as the two modes move apart - thus reducing fringe contrast - and then back together, due to the trap potential.

The data shown in Figure 4 gives the value of the two-mode moment as $|\langle \hat{a}^\dagger \hat{b} \rangle| = 20,000$. Using the bound $n_{st} \geq 2|\langle \hat{a}^\dagger \hat{b} \rangle|$, this implies a depth of mode steering (and entanglement) of at least $n_{st} = 40,000$ atoms. Moreover, using the criterion based on $|\langle \hat{a}^\dagger \hat{b} \rangle|$, we see the steering is “two-way”. We thus demonstrate the steering of an atomic system of at least 20,000 atoms, by another.

Finally, we note that in the experiment the two condensate modes spatially separate at time $T \sim 0.2s$, due to the excitation of collective oscillations [29, 30], before being brought back together with minimal loss of quantum coherence and a revival of interference contrast, at $T \sim 0.35s$. A similar spontaneous separation of two-mode functions and associated revival of the Ramsey contrast has been recently reported in a BEC interferometer with

5000 atoms [63], to give evidence of spin squeezing. Assuming mechanisms for decoherence with spatial separation of the modes would likely destroy EPR correlations irreversibly, these results are promising that mesoscopic EPR steering correlations will be detected at full spatial separation of the modes. Magnetic fields could be used to achieve greater spatial separations, since the modes correspond to different spin states.

This research has been supported by the Australian Research Council Discovery Project Grants schemes under Grant DP140104584 and DP180102470. This work was performed in part at Aspen Center for Physics, which is supported by National Science Foundation grant PHY-1607611. BD thanks the Centre for Cold Matter, Imperial College for hospitality during this research. We thank V. Ivannikov and M. Egorov for assistance with obtaining experimental data.

-
- [1] A. Einstein, B. Podolsky and N. Rosen, *Phys. Rev.* **47**, 777 (1935).
 - [2] E. Schrödinger, *Proc. Camb. Phil. Soc.* **31**, 555 (1935).
 - [3] H. M. Wiseman, S. J. Jones and A. C. Doherty, *Phys. Rev. Lett.* **98**, 140402 (2007).
 - [4] S. J. Jones, H. M. Wiseman and A. Doherty, *Phys. Rev. A* **76**, 052116 (2007).
 - [5] E. G. Cavalcanti, S. J. Jones, H. M. Wiseman and M. D. Reid, *Phys. Rev. A* **80**, 032112 (2009).
 - [6] M. D. Reid, *Phys. Rev. A* **40**, 913 (1989).
 - [7] M. D. Reid, P. D. Drummond, W. P. Bowen, E. G. Cavalcanti, P. K. Lam, H. A. Bachor, U. L. Andersen and G. Leuchs, *Rev. Mod. Phys.* **81**, 1727 (2009).
 - [8] D. J. Saunders, S. J. Jones, H. M. Wiseman and G. J. Pryde, *Nature Physics* **6**, 845 (2010).
 - [9] W. H. Furry, *Phys. Rev.* **49**, 393 (1936).
 - [10] A. Bassi, K. Lochan, S. Satin, T. P. Singh and H. Ulbricht, *Rev. Mod. Phys.* **85**, 471 (2013).
 - [11] J. Peise, I. Kruse, K. Lange, B. Lücke, L. Pezzè, J. Arlt, W. Ertmer, K. Hammerer, L. Santos, A. Smerzi and C. Klempt, *Nature Communications* **6**, 8984 (2015).
 - [12] R. Schmied, J.-D. Bancal, B. Allard, M. Fadel, V. Scarani, P. Treutlein and N. Sangouard, *Science* **352**, 441 (2016).
 - [13] N. J. Engelsens, R. Krishnakumar, O. Hosten and M. A. Kasevich, *Phys. Rev. Lett.* **118**, 140401 (2017).
 - [14] P. Kunkel, M. Prüfer, H. Strobel, D. Linnemann, A. Frölian, T. Gasenzer, M. Gärtner and M. K. Oberthaler, *Science* **360**, 413 (2018).
 - [15] M. Fadel, T. Zibold, B. Décamps and P. Treutlein, *Science* **360**, 409 (2018).
 - [16] R. Riedinger, A. Wallucks, I. Marinković, C. Löschnauer, M. Aspelmeyer, S. Hong, and S. Gröblacher, *Nature* **556**, 473 (2018).
 - [17] C. F. Ockeloen-Korppi, E. Damskägg, J.-M. Pirkkalainen, M. Asjad, A. A. Clerk, F. Massel, M. J. Woolley, and M. A. Sillanpää, *Nature* **556**, 478 (2018).
 - [18] C. Gross, H. Strobel, E. Nicklas, T. Zibold, N. Bar-Gill, G. Kurizki and M. K. Oberthaler, *Nature* **480**, 219 (2011).

- (2011).
- [19] K. Lange, J. Peise, B. Lücke, I. Kruse, G. Vitagliano, I. Apellaniz, M. Kleinmann, G. Tóth and C. Klempt, *Science* **360**, 416 (2018).
- [20] J. S. Bell, *Physics* **1**, 195 (1964).
- [21] C. Branciard, E. G. Cavalcanti, S. P. Walborn, V. Scarani, and H. M. Wiseman, *Phys. Rev. A* **85**, 010301(R) (2012). Q. He, L. Rosales-Zarate, G. Adesso, and M Reid, *Phys. Rev. Lett.* **115**, 180502 (2015). M. D Reid, *Phys. Rev. A* **88**, 062338 (2013). T. Wasak and J. Chwedeńczuk, *Phys. Rev. Lett.* **120**, 140406 (2018).
- [22] I. Marinković, A. Wallucks, R. Riedinger, S. Hong, M. Aspelmeyer, and S. Gröblacher, *Phys. Rev. Lett.* **121**, 220404 (2018).
- [23] A. S. Sørensen and K. Mølmer, *Phys. Rev. Lett.* **86**, 4431 (2001).
- [24] L. Rosales-Zárate, B. Dalton, and M. Reid, *Phys. Rev. A* **98**, 022120 (2018).
- [25] C. Gross, T. Zibold, E. Nicklas, J. Esteve, and M. K. Oberthaler, *Nature (London)* **464**, 1165 (2010).
- [26] M. F. Riedel, P. Böhi, Y. Li, T. W. Hänsch, A. Sinatra, and P. Treutlein, *Nature (London)* **464**, 1170 (2010).
- [27] R. McConnell, H. Zhang, J. Hu, S. Cuk, and V. Vuletic, *Nature* **519**, 439 (2015).
- [28] F. Fröwis, P. C. Strassmann, A. Tiranov, C. Gut, J. Lavoie, N. Brunner, F. Bussièeres, M. Afzelius and N. Gisin, *Nature Communications* **8**, 907 (2017).
- [29] M. Egorov, R. P. Anderson, V. Ivannikov, B. Opanchuk, P. Drummond, B. V. Hall and A. I. Sidorov, *Phys. Rev. A* **84**, 021605 (2011).
- [30] M. Egorov, B. Opanchuk, P. D. Drummond, B. V. Hall, P. Hannaford, and A. I. Sidorov, *Phys. Rev. A* **87**, 053614 (2013).
- [31] H. M. Wiseman and J. A. Vaccaro, *Phys. Rev. Lett.* **91**, 097902 (2003).
- [32] N. Killoran, M. Cramer, and M. B. Plenio, *Phys. Rev. Lett.* **112**, 150501 (2014).
- [33] B. J. Dalton, J. Goold, B. M. Garraway, and M. D. Reid, *Physica Scripta* **92**, 023004 (2017). B. J. Dalton, J. Goold, B. M. Garraway, and M. D. Reid (2017); *ibid*, *Physica Scripta* **92**, 023004 (2017).
- [34] B. J. Dalton, L. Heaney, J. Goold, B. M. Garraway, and Th. Busch, *New J. Phys.*, **16**, 013026 (2014).
- [35] G. C. Wick, A. S. Wightman, and E. P. Wigner, *Phys. Rev.* **88**, 101 (1952).
- [36] S. Bartlett, T. Rudolph, and R. Spekkens, *Rev. Mod. Phys.* **79**, 555 (2007).
- [37] M. R. Dowling, S. D. Bartlett, T. Rudolph, and R. W. Spekkens, *Phys. Rev. A* **74**, 052113 (2006).
- [38] J. Bancal, N. Gisin, Y. C. Liang, and S. Pironio, *Phys. Rev. Lett.* **106**, 250404 (2011).
- [39] Q. Y. He and M. D. Reid, *Phys Rev Lett.* **111**, 250403 (2013).
- [40] See Supplemental Materials for the proof of the pseudo-label N -partite entanglement and N -partite steering of the two-mode state (1), the derivation of the entropy of entanglement for the two-mode state, the derivation of the criterion for depth of steering, a description of the BEC interferometer, and of the three-dimensional multi-mode model.
- [41] S. Yu, Q. Cheng, C. Zhang, C. H. Lai, and C. H. Oh, *Phys. Rev. Lett.* **109**, 120402 (2012).
- [42] P. Zanardi, *Phys. Rev. A* **65**, 042101 (2002). H. Barnum, E. Knill, G. Ortiz, R. Somma, and L. Viola, *Phys. Rev. Lett.* **92**, 107902 (2004).
- [43] M. S. Kim, W. Son, V. Bužek, and P. L. Knight, *Phys. Rev. A* **65**, 032323 (2002).
- [44] Y. Li, Y. Castin, and A. Sinatra, *Phys. Rev. Lett.* **100**, 210401 (2008).
- [45] Y. Li, P. Treutlein, J. Reichel, and A. Sinatra. *Eur. Phys. J. B* **68**, 365 (2009).
- [46] J. Estève, C. Gross, A. Weller, S. Giovanazzi, and M. K. Oberthaler, *Nature* **455**, 1216 (2008).
- [47] Q. Y. He, P. D. Drummond, M. K. Olsen, and M. D. Reid, *Phys. Rev. A* **86**, 023626 (2012).
- [48] B. Opanchuk, Q. Y. He, M. D. Reid, and P. D. Drummond, *Phys. Rev. A* **86**, 023625 (2012).
- [49] M. Hillery and M. S. Zubairy, *Phys. Rev. Lett.* **96**, 050503 (2006).
- [50] E. G. Cavalcanti, Q. Y. He, M. D. Reid, and H. M. Wiseman, *Phys. Rev. A* **84**, 032115 (2011).
- [51] B. J. Dalton, B. Garraway, and M. D. Reid, *quant-ph arXiv*: 1611.09101.
- [52] C. Deutsch, F. Ramirez-Martinez, C. Lacroûte, F. Reinhard, T. Schneider, J. N. Fuchs, F. Piéchon, F. Laloë, J. Reichel, and P. Rosenbusch, *Phys. Rev. Lett.* **105**, 020401(2010).
- [53] K. S. Hardman, P. B. Wigley, P. J. Everitt, P. Manju, C. C. N. Kuhn, and N. P. Robins, *Opt. Lett.* **41**, 2505 (2016).
- [54] O. Penrose and L. Onsager, *Phys. Rev.* **104**, 576 (1956).
- [55] B. Opanchuk, M. Egorov, S. Hoffmann, A. Sidorov, and P. Drummond, *Europhys. Lett.*, **97**, 50003 (2012).
- [56] A. Widera, F. Gerbier, S. Fölling, T. Gericke, O. Mandel, and I. Bloch, *PNew J. Phys.* **8**, 152 (2006).
- [57] K. M. Mertes, J. W. Merrill, R. Carretero-González, D. J. Frantzeskakis, P. G. Kevrekidis, and D. S. Hall, *Phys. Rev. Lett.* **99**, 190402 (2007).
- [58] Markus Holzmann, Werner Krauth, and Martin Naraschewski, *Phys. Rev. A* **59**, 2956 (1999).
- [59] F. Gerbier, J. H. Thywissen, S. Richard, M. Hugbart, P. Bouyer, and A. Aspect, *Phys. Rev. A* **70**, 013607 (2004).
- [60] B. Opanchuk and P. D. Drummond, *J. Math. Phys.* **54**(4), 042107 (2013).
- [61] P. D. Drummond and A. D. Hardman, *Europhys. Letters* **21**, 279 (1993).
- [62] M. J. Steel, M. K. Olsen, L. I. Plimak, P. D. Drummond, S. M. Tan, M. J. Collett, D. F. Walls, and R. Graham, *Phys. Rev. A* **58**, 4824 (1998).
- [63] T. Laudat, V. Dugrain, T. Mazzoni, M.-Z. Huang, C. L. Garrido Alzar, A. Sinatra, P. Rosenbusch, and J. Reichel, *arXiv*:1804.07536